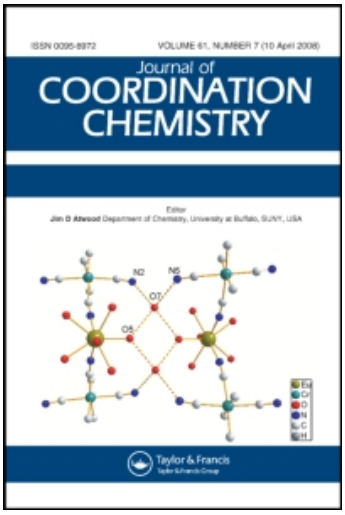

Journal of Coordination Chemistry
Publication details, including instructions for authors and subscription information:
http://www.informaworld.com/smpp/title~content=t713455674

Synthesis and characterization of the organoimidopolyoxomolybdates [n-$Bu_4N]_2[Mo_6O_{17}(\equiv NAr)_2]$ (Ar = 2-ethyl-6-methylphenyl and 2-isopropyl-6-methylphenyl)

Yapeng Shi[a]; Ganglin Xue[a]; Huaiming Hu[a]; Feng Fu[b]; Jiwu Wang[b]
[a] Department of Chemistry, Northwest University, People's Republic of China [b] Department of Chemistry, Yanan University, People's Republic of China

To cite this Article Shi, Yapeng , Xue, Ganglin , Hu, Huaiming , Fu, Feng and Wang, Jiwu(2006) 'Synthesis and characterization of the organoimidopolyoxomolybdates [n-$Bu_4N]_2[Mo_6O_{17}(\equiv NAr)_2]$ (Ar = 2-ethyl-6-methylphenyl and 2-isopropyl-6-methylphenyl)', Journal of Coordination Chemistry, 59: 15, 1739 — 1747
To link to this Article: DOI: 10.1080/00958970500537978
URL: http://dx.doi.org/10.1080/00958970500537978

Journal of Coordination Chemistry
Vol. 59, No. 15, 15 October 2006, 1739–1747

Synthesis and characterization of the organoimidopolyoxomolybdates $[n\text{-}Bu_4N]_2[Mo_6O_{17}(\equiv NAr)_2]$ (Ar = 2-ethyl-6-methylphenyl and 2-isopropyl-6-methylphenyl)

YAPENG SHI†, GANGLIN XUE*†, HUAIMING HU†,
FENG FU‡ and JIWU WANG‡

†Department of Chemistry, Northwest University, Shaanxi Key Laboratory of Physical Inorganic Chemistry, Xi'an 710069, People's Republic of China
‡Department of Chemistry, Yanan University, Xi'an 716000, People's Republic of China

(*Received in final form 26 October 2005*)

Two new bifunctionalized arylimido derivatives of hexamolybdate, $[n\text{-}Bu_4N]_2[Mo_6O_{17}(C_6H_3N\text{-}2\text{-}C_2H_5\text{-}6\text{-}CH_3)_2]$ **(1)** and $[n\text{-}Bu_4N]_2[Mo_6O_{17}(C_6H_3N\text{-}2\text{-}CH(CH_3)_2\text{-}6\text{-}CH_3)_2]\cdot H_2O$ **(2)**, in which the two organoimido groups are covalently bonded to hexamolybdate at the *cis* positions, were synthesized by self-assembled metathesis of α-octamolybdate and organoimido ligands with *N*,*N*′-dicyclohexylcarbodiimide as dehydration agent, and characterized by elemental analysis, ^{1}H NMR, IR and electronic spectroscopy, and X-ray diffraction analysis. Both derivatives have short Mo–N bond distances [Mo(1)–N(1), 1.740(3) Å; Mo(2)–N(2), 1.739(3) Å for **1** and Mo(1)–N(1), 1.734(3) Å; Mo(2)–N(2), 1.741(3) Å for **2**] and form dimers via π–π stacking in the crystalline state.

Keywords: Polyoxometalates; Organoimido derivatives; Crystal structures

1. Introduction

Polyoxometalates (POMs) represent an immense class of metal–oxygen cluster compounds characterized by fascinating structural, electrochemical, catalytic, magnetic, medicinal and photophysical properties, in both the solid state and solution [1]. Because of so-called value-adding properties and possible synergistic effects, organically derived POMs have attracted considerable attention and now constitute a significant area of research [2]. Among the many organic derivatives of POMs, organoimido derivatives have attracted particular interest because the organic π electrons may extend their conjugation to the inorganic framework, thus resulting in strong d–π interactions. Great effort has been directed towards the functionalization of POM clusters, particularly the hexamolybdate ion, in which the six terminal oxygen ligands can be partially or completely replaced with organoimido ligands [3–12]. Here we report the synthesis,

*Corresponding author. Email: xglin707@163.com

ISSN 0095-8972 print/ISSN 1029-0389 online © 2006 Taylor & Francis
DOI: 10.1080/00958970500537978

structure and characterization of two new difunctionalized hexamolybdates $[Mo_6O_{17}(\equiv NAr)_2]^{2-}$ (Ar = 2-ethyl-6-methylphenyl and 2-isopropyl-6-methylphenyl).

2. Experimental

2.1. *Materials and measurements*

$[n\text{-}Bu_4N]_4[\alpha\text{-}Mo_8O_{26}]$ was prepared by literature methods [13]. Acetonitrile was dried by refluxing over P_2O_5 and distilled prior to use. C, H and N were determined by a PE 240Q elemental analyzer. IR spectra (4000–400 cm^{-1}; KBr pellets) were recorded with an EQUINOX55 spectrophotometer. ^1H NMR spectra were obtained using an INOVA-400 NMR spectrometer with acetone-d_6 as solvent and Me_4Si as internal standard. Electronic spectra were recorded on a Shimadzu UV2550 spectrophotometer.

2.2. *[n-Bu_4N]$_2$[$Mo_6O_{17}(C_6H_3N$-2-C_2H_5-6-$CH_3)_2$] (1) and [n-Bu_4N]$_2$[$Mo_6O_{17}(C_6H_3N$-2-$CH(CH_3)_2$-6-$CH_3)_2$]·H_2O (2)*

A typical synthesis is as follows for **1**. A mixture of 2-ethyl-6-methylaniline (0.1352 g, 1.0 mmol), *N*,*N*′-dicyclohexylcarbodiimide (0.21 g, 1.0 mmol), and $[n\text{-}Bu_4N]_4[\alpha\text{-}Mo_8O_{26}]$ (1.17 g, 0.5 mmol) was refluxed in anhydrous acetonitrile (15 cm^3) under nitrogen for about 24 h. After being cooled to room temperature, filtration of the resulting dark-red solution removed a white precipitates. The product precipitated from the filtrate as orange-red crystals. It was collected by filtration, washed successively with EtOH and Et_2O several times, and then recrystallized twice from acetone to yield 0.54 g of **1** (yield based on Mo: 67%). Anal. Calcd for $C_{50}H_{94}N_4O_{17}Mo_6$ (%): C, 37.56; H, 5.93; N, 3.50. Found: C, 37.49; H, 5.84; N, 3.54. IR (cm^{-1}): 1475(s), 1381(m), 1322(m), 934(s), 782(vs), 633(m). ^1H NMR (400 MHz, 25°C): $\delta = 6.99$ (d, ArH, 2H), 6.97 (d, ArH, 2H), 6.82 (t, ArH, 2H), 3.42 (t, NCH_2, $[n\text{-}Bu_4N]^+$, 16H), 3.01 (q, CH_2, 4H), 2.61 (s, (Ar-)CH_3, 6H), 1.79 (m, CH_2, $[n\text{-}Bu_4N]^+$, 16H), 1.42 (m, CH_2, $[n\text{-}Bu_4N]^+$, 16H), 1.27 (t, (Ar−)CH_2Me, 6H), 0.94 ppm (t, CH_3, $[n\text{-}Bu_4N]^+$, 24 H). Electronic spectrum (MeCN): $\lambda_{max} = 242$, 354 nm. A similar procedure furnished **2** as red crystals (yield, 64%). Anal. Calcd for $C_{52}H_{100}N_4O_{18}Mo_6$ (%): C, 39.97; H, 6.12; N, 3.41. Found: C, 38.24; H, 5.94; N, 3.53. IR (cm^{-1}): 1474(s), 1379(m), 1341(m), 1308(m), 943(vs), 777(vs), 592(m). ^1H NMR: $\delta = 7.07$ (d, ArH, 2H), 6.99 (d, ArH, 2H), 6.87 (t, ArH, 2H), 3.94 (m CH, 2H), 3.43 (t, NCH_2, $[n\text{-}Bu_4N]^+$, 16H), 2.65 (s, (Ar–)CH_3, 6 H), 1.79 (m, CH_2, $[n\text{-}Bu_4N]^+$, 16H), 1.43 (m, CH_2, $[n\text{-}Bu_4N]^+$, 16H), 1.28 (s, (Ar–)CHMe_2, 12H), 0.94 ppm (t, CH_3, $[n\text{-}Bu_4N]^+$, 24H). Electronic spectrum (MeCN): $\lambda_{max} = 242$, 352 nm.

Crystals suitable for single-crystal X-ray analysis were grown by diffusion of Et_2O into an acetonitrile solution at room temperature. Both **1** and **2** are all highly soluble in many common organic solvents including acetone, acetonitrile and *N*,*N*′-dimethyl formamide.

2.3. *X-ray crystallography*

An orange-red crystal of **1** and a red crystal of **2** were respectively mounted on glass fibre capillaries on a Bruker SMART APEX II CCD diffractometer equipped with

graphite-monochromatised radiation. Data were collected at 273(2) K using Mo-Kα radiation ($\lambda = 0.71073$ Å). The structures were solved by direct methods (SHELXTL-97) and refined by the full-matrix least-squares method on F^2. Anisotropic temperature factors were applied to all non-hydrogen atoms. A summary of crystal data, experimental details, and refinement results for the structures of **1** and **2** is given in table 1. Selected bond lengths and angles are given in tables 2 and 3.

3. Results and discussion

3.1. *Structures of $[Mo_6O_{17}(\equiv NAr)_2]^{2-}$ (1 and 2)*

Both **1** and **2** crystallize in the triclinic space group $P\bar{1}$ and possess very similar molecular structures; an ORTEP diagrams of the $[Mo_6O_{17}(\equiv NAr)_2]^{2-}$ anion is shown in figure 1. Contrary to expectations based on steric considerations, **1** and **2** adopt a *cis* structure with the imido groups occupying adjacent terminal positions on the hexamolybdate cage as the difunctionalized hexamolybdates, which shows that the presence of one imido substituent exerts an activating effect at proximal oxo sites. Its metrical parameters [Mo(1)–N(1), 1.740(3), Mo(2)–N(2), 1.739(3) Å, Mo(1)–N(1)–C(1), 175.4(4), Mo(2)–N(2)–C(11), 173.9(4)° for **1** and Mo(1)–N(1), 1.734(3), Mo(2)–N(2),

Table 1. Summary of crystal data and structure refinement details for the *bis*-imidohexamolybdates.

	1	**2**
Empirical formula	$C_{50}H_{94}Mo_6N_4O_{17}$	$C_{52}H_{98}Mo_6N_4O_{18}$
Formula weight	1598.94	1642.98
Temperature (K)	273(2)	273(2)
Wavelength (Å)	0.71073	0.71073
Crystal system	Triclinic	Triclinic
Space group	$P\bar{1}$	$P\bar{1}$
a (Å)	12.736(3)	12.769(1)
b (Å)	12.811(3)	12.833(1)
c (Å)	20.818(5)	21.381(2)
α (°)	84.421(2)	82.946(2)
β (°)	78.720(2)	86.101(2)
γ (°)	76.055(2)	78.504(2)
Volume (Å^3)	3228.41(13)	3404(6)
Z	1	1
D_{calcd} (g cm^{-3})	0.822	0.8014
Absorption coefficient (mm^{-1})	0.597	0.568
F(000)	810	834
Crystal size (mm^3)	$0.32 \times 0.30 \times 0.24$	$0.48 \times 0.46 \times 0.32$
θ range for data collection (°)	2.59 to 29.75	1.80 to 29.13
Index ranges	$-17 \le h \le 17$, $-16 \le k \le 17$, $-28 \le l \le 28$	$-17 \le h \le 13$, $-17 \le k \le 14$, $-28 \le l \le 28$
Reflections collected	33,132	21,642
Reflections unique	17,665 [R(int) = 0.0350]	15,824 [R(int) = 0.0155]
Refinement method	Full-matrix least-squares on F^2	Full-matrix least-squares on F^2
Data/restraints/parameters	17,665/0/706	15,824/0/730
Goodness-of-fit on F^2	0.874	1.020
Final R indices [$I > 2\sigma(I)$]	$R_1 = 0.0424$, $wR_2 = 0.1080$	$R_1 = 0.0344$, $wR_2 = 0.0917$
R indices (all data)	$R_1 = 0.0963$, $wR_2 = 0.1294$	$R_1 = 0.0559$, $wR_2 = 0.0975$
Largest diff. peak and hole (e Å^{-3})	0.802 and −0.721	0.770 and −0.538

Table 2. Selected bond lengths (Å) and angles (°) for **1**.

Mo(1)–N(1)	1.740(3)
Mo(1)–O(11)	1.906(3)
Mo(1)–O(7)	1.918(3)
Mo(1)–O(2)	1.967(3)
Mo(1)–O(17)	2.005(3)
Mo(1)–O(1)	2.234(2)
Mo(3)–O(3)	1.684(3)
Mo(3)–O(2)	1.890(3)
Mo(3)–O(8)	1.918(3)
Mo(3)–O(16)	1.928(3)
Mo(3)–O(13)	1.937(3)
Mo(3)–O(1)	2.384(2)
Mo(5)–O(5)	1.698(3)
Mo(5)–O(17)	1.862(3)
Mo(5)–O(14)	1.908(3)
Mo(5)–O(16)	1.934(3)
Mo(5)–O(15)	1.972(3)
Mo(5)–O(1)	2.338(2)
O(11)–Mo(1)–O(7)	90.50(12)
O(11)–Mo(1)–O(2)	156.34(12)
O(7)–Mo(1)–O(2)	87.31(12)
O(11)–Mo(1)–O(17)	87.09(11)
O(7)–Mo(1)–O(17)	155.67(12)
O(2)–Mo(1)–O(17)	85.32(12)
O(11)–Mo(1)–O(1)	77.74(10)
O(7)–Mo(1)–O(1)	78.84(10)
O(2)–Mo(1)–O(1)	78.72(10)
O(17)–Mo(1)–O(1)	76.99(10)

Table 3. Selected bond lengths (Å) and angles (°) for **2**.

Mo(1)–N(1)	1.734(3)
Mo(1)–O(11)	1.930(2)
Mo(1)–O(7)	1.934(2)
Mo(1)–O(2)	1.970(2)
Mo(1)–O(17)	1.982(2)
Mo(1)–O(1)	2.2311(17)
Mo(3)–O(3)	1.686(2)
Mo(3)–O(2)	1.880(2)
Mo(3)–O(8)	1.912(2)
Mo(3)–O(13)	1.935(2)
Mo(3)–O(16)	1.935(2)
Mo(3)–O(1)	2.3762(17)
Mo(5)–O(5)	1.692(2)
Mo(5)–O(17)	1.878(2)
Mo(5)–O(16)	1.926(2)
Mo(5)–O(16)	1.929(2)
Mo(5)–O(15)	1.960(2)
Mo(5)–O(1)	2.3480(18)
O(11)–Mo(1)–O(7)	89.65(9)
O(11)–Mo(1)–O(2)	156.05(8)
O(7)–Mo(1)–O(2)	87.65(9)
O(11)–Mo(1)–O(17)	87.39(9)
O(7)–Mo(1)–O(17)	155.30(8)
O(2)–Mo(1)–O(17)	85.22(9)
O(11)–Mo(1)–O(1)	77.81(7)
O(7)–Mo(1)–O(1)	78.46(7)
O(2)–Mo(1)–O(1)	78.33(7)
O(17)–Mo(1)–O(1)	76.94(7)

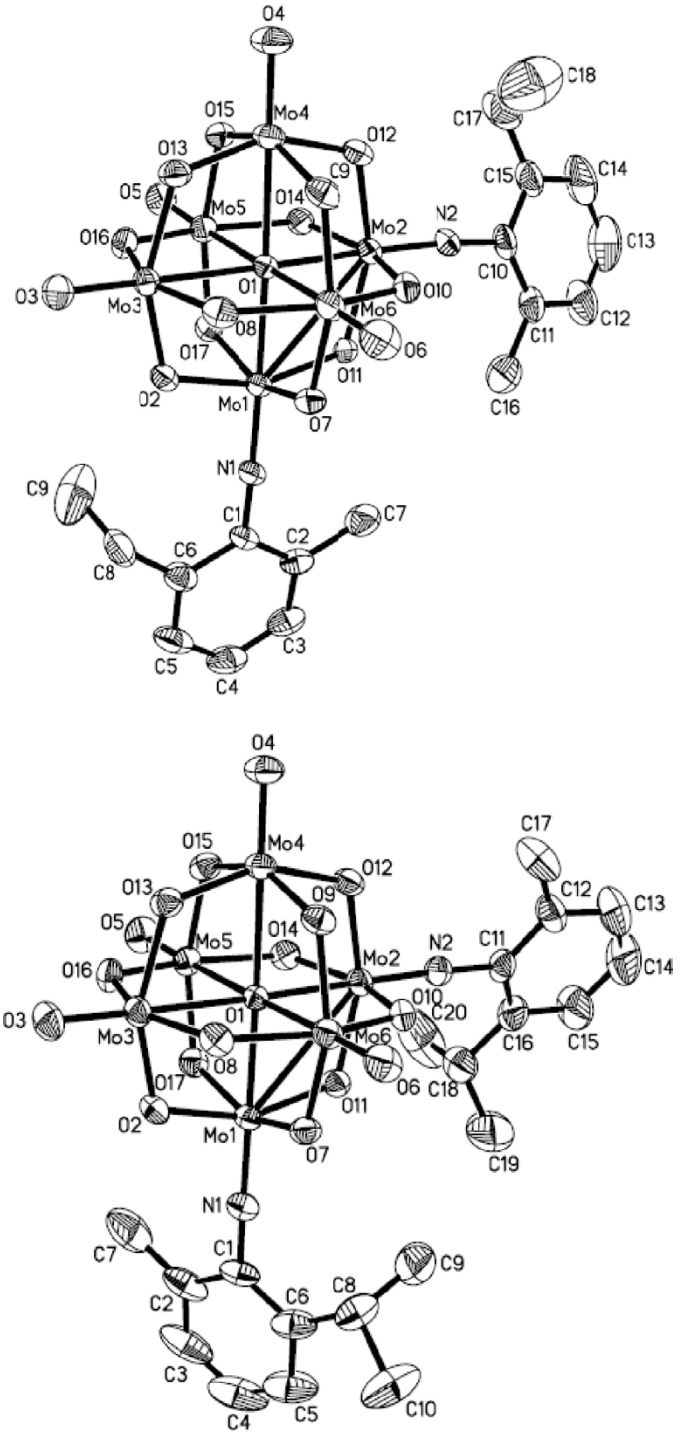

Figure 1. ORTEP representation of the difunctionalized hexamolybdate anions within **1** (upper) and **2** (lower) with displacement ellipsoids drawn at the 30% probability level. H atoms have been omitted for clarity.

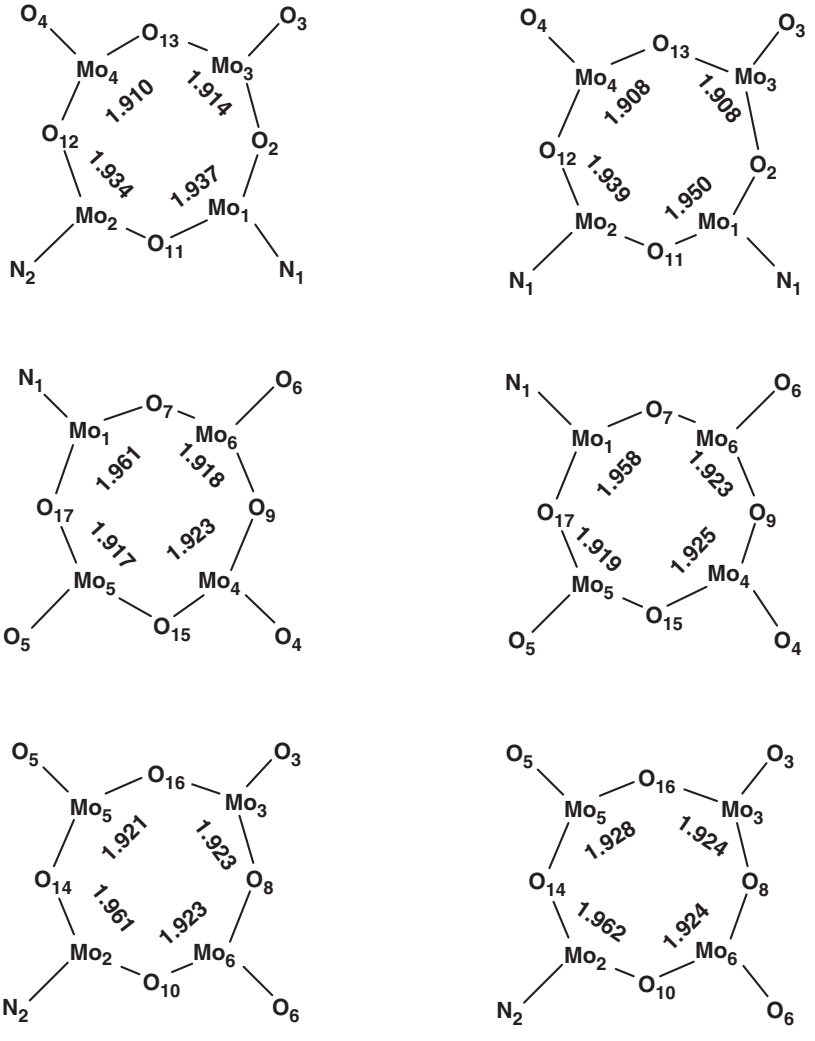

Figure 2. Comparison of average {Mo–O_b} distances (Å) at the [Mo=NAr] and [Mo=O] sites, within the complementary $\{Mo_4(O_b)_4\}$ belts of **1** (left) **2** (right).

1.741(3) Å, Mo(1)–N(1)–C(1), 174.1(2), Mo(2)–N(2)–C(11), 174.7(3)° for **2**] indicate substantial [Mo≡NAr] triple bond character [14]. The central oxygen atom inside the hexamolybdate cage is drawn closer to the imido-bearing Mo atom, while the four bridge oxygen atoms are pushed away. Along the Mo(1)–O(1)–Mo(4) axis, the central O(1) atom is substantially nearer to the imido-bearing Mo(1) site [2.234(2) Å for **1**, 2.231(2) Å for **2**] than to the *trans* oxo Mo(4) site [2.366(2) Å for **1**, 2.378(2) Å for **2**]. This distortion has been attributed to the greater *trans*-influence of the terminal oxo ligand relative to the imido ligand [8]. Figure 2 presents the Mo–O_b distances in the $[Mo_4(O_b)_4]$ belts of both **1** and **2**. Obviously, Mo–O_b bond lengths are generally longer at [Mo≡NAr] sites than at [Mo≡O] sites. It is known that among all the oxygen atoms in an $[Mo_6O_{19}]^{2-}$ anion, the double bridge oxygen atoms have the highest negative charge density [15]. The charge density on the double bridge oxygen

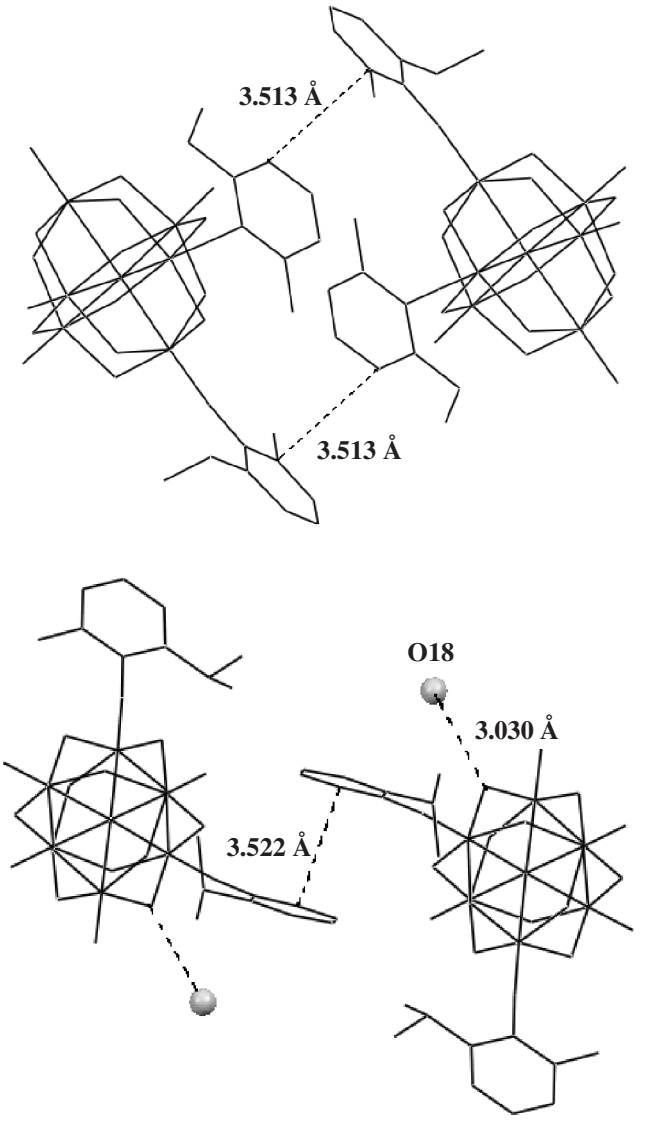

Figure 3. Dimer formation of the anions in the lattice of **1** (up) and **2** (bottom).

atom can be further increased by the electron donating effect of the two organoimido ligands [16].

While compounds **1** and **2** show very similar molecular structures, their crystal-packing motifs are rather different (figure 3). In the lattices of **1** and **2**, the cluster ions are organized into dimers. The "dimerization" in **1** is facilitated by two pairs of π–π stacks of parallel phenyl rings, the existence of the π–π interactions being clearly indicated by the separation of 3.513 Å. Such "dimerization" is also observed in the crystal structure of **2**, but there exists only one pair of π–π stacks of phenyl rings, and the separation between the two rings is 3.522 Å. In addition, a molecule of water in **2**

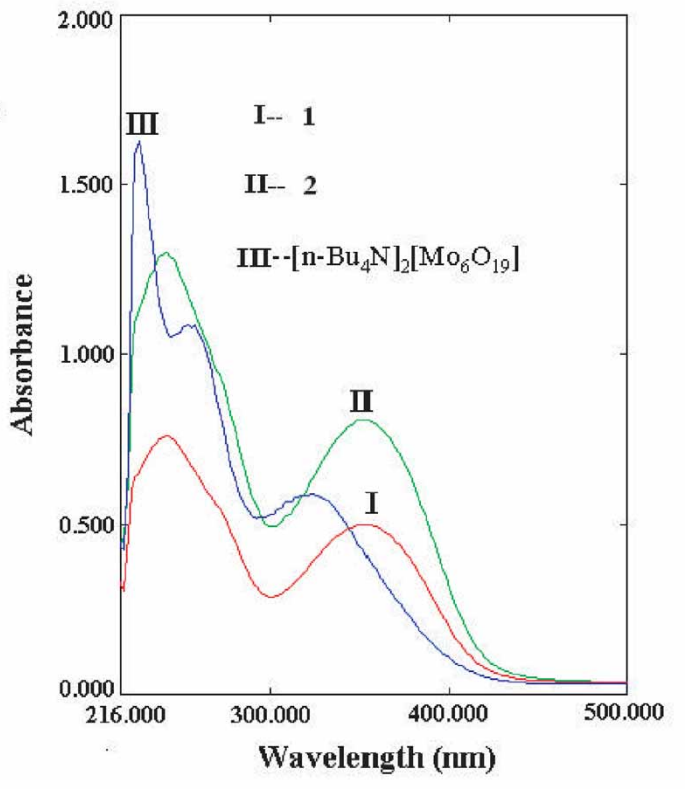

Figure 4. Electronic spectra of $[n\text{-}Bu_4N]_2[Mo_6O_{19}]$, **1** and **2**.

forms a hydrogen bond with O(2) of a neighboring hexamolybdate cage with a distance of 3.030 Å.

3.2. *Spectroscopic studies*

^{1}H NMR spectra showed clearly resolved signals which could all be unambiguously assigned. The integration matches well with the proposed structure. Compared to ^{1}H NMR spectra of the corresponding free amine ligand, except for those in the tetrabutylammonium counterions, all protons exhibit larger chemical shifts after imido bond formation, indicating the much weaker shielding nature of $[Mo_5O_{17}(Mo{\equiv}N-)_2]^{2-}$ than the amino. For example, the aromatic doublets shifts from 6.95 and 7.04 to 6.99 and 7.07 ppm, while the methyl resonance shifts from 2.18 to 2.65 ppm in **2**. Such a shift is consistent with the electron-withdrawing nature of the Mo≡N triple bond.

IR spectra are similar to those of previously reported *cis*-bifunctionalized organoimido derivatives [7, 8, 11, 12]. They closely resemble that of the hexamolybdate parent in that there are the very strong bands, $\nu(Mo{=}O_t)$, $\nu(Mo{-}O_b{-}Mo)$ and $\nu(Mo{-}O_c{-}Mo)$, at ca 941 and 777 cm^{-1} for **1**, and 943 and 777 cm^{-1} for **2**, respectively.

In electronic spectra (figure 4), the lowest energy electronic transition at 325 nm in $[Mo_6O_{19}]^{2-}$ was assigned to a charge-transfer transition from the oxygen π-type non-bonding HOMO to the molybdenum π-type LUMO, which is bathochromically shifted by more than 25 nm and becomes considerably more intense in **1** (354 nm) and **2** (352 nm). This indicates that the Mo–N π-bond is delocalized with the organic conjugated π-electrons [3]. In other words, there is a strong electronic interaction between the metal oxygen cluster and the organic conjugated ligands.

Supplementary material

Crystallographic data for the structural analysis have been deposited with the Cambridge Crystallographic Data Centre, CCDC 280245 for **1** and CCDC 280246 for **2**. Copies may be obtained free of charge from The Director, CCDC, 12 Union Road, Cambridge, CB2 IEZ, UK (Fax: +44-1223-336033; E-mail: deposit@ccdc.cam.ac.uk or www.http://www.ccde.cam.ac.uk).

Acknowledgements

We sincerely thank the Education Commission of Shaanxi Province (03JK077, 03JS006) and the Natural Science Foundation of Shaanxi Province (2003B01) for support of this work.

References

[1] M.T. Pope. *Heteropoly and Isopoly Oxometalates*, Springer-Verlag, New York (1983); M.T. Pope, A. Müller. *Angew. Chem. Int. Ed. Engl.*, **30**, 34 (1991); M.T. Pope and A. Müller (Eds). *Polyoxometalates: From Platonic Solids to Anti-Retroviral Activity*, Kluwer, Dordrecht (1994); C.L. Hill. *Chem. Rev.*, **98**, 1 (1998).
[2] P. Gouzerh, A. Proust. *Chem. Rev.*, **98**, 77 (1998).
[3] Y. Du, A.L. Rheingold, E.A. Maatta. *J. Am. Chem. Soc.*, **114**, 345 (1992).
[4] J.L. Stark, A.L. Rheingold, E.A. Maatta. *J. Chem. Soc., Chem. Commun.*, 1165 (1995).
[5] J.L. Stark, V.G. Young, E.A. Maatta. *Angew. Chem. Int. Ed. Engl.*, **34**, 2547 (1995).
[6] J.B. Strong, B.S. Haggerty, A.L. Rheingold, E.A. Maatta. *J. Chem. Soc., Chem. Commun.*, 1137 (1997).
[7] J.B. Strong, R. Ostrander, A.L. Rheingold, E.A. Maatta. *J. Am. Chem. Soc.*, **116**, 3601(1994); J.B. Strong, G.P.A. Yap, R. Ostrander, L.M. Liable-Sands, A.L. Rheingold, R. Thouvenot, P. Gouzerh, E.A. Maatta. *J. Am. Chem. Soc.*, **122**, 639 (2000).
[8] A. Proust, R. Thouvenot, M. Chaussade, F. Robert, P. Gouzerh. *Inorg. Chim. Acta*, **224**, 81 (1994).
[9] W. Clegg, R.J. Errington, K.A. Fraser, C. Lax, D.G. Richards. In *Polyoxometalates: From Platonic Solids to Anti-Retroviral Activity*, M.T. Pope, A. Müller (Eds), p. 113, Kluwer, Dordrecht (1994).
[10] W. Clegg, R.J. Errington, K. Fraser, S.A. Holmes, A. Schäfer. *J. Chem. Soc., Chem. Commun.*, 455 (1995).
[11] L. Xu, M. Lu, B. Xu, Y. Wei, Z. Peng, D.R. Powell. *Angew. Chem.*, **114**, 4303 (2002); *Angew. Chem. Int. Ed.*, **41**, 4129 (2002); Z. Peng. *Angew. Chem. Int. Ed.*, **43**, 930 (2004).
[12] Q. Li, P. Wu, Y. Wei, Y. Wang, P. Wang, H. Guo. *Inorg. Chem. Commun.*, **7**, 524 (2004).
[13] J. Fuchs, H. Hartl. *Angew. Chem. Int. Ed. Engl.*, **15**, 375 (1976); W.G. Klemperer, W. Shum. *J. Am. Chem. Soc.*, **98**, 8291 (1976).
[14] D.E. Wigley. *Prog. Inorg. Chem.*, **42**, 239 (1994).
[15] A.J. Bridgeman, G. Cavigliasso. *Inorg. Chem.*, **41**, 1761 (2002).
[16] J.L. Stark, V.G. Young, E.A. Maatta. *Angew. Chem.*, **107**, 2751 (1995); *Angew. Chem. Int. Ed. Engl.*, **34**, 2547 (1995).